

1 **Future Projections of Extreme Storm Tides and Related Coastal Flooding**
2 **along the Greek Coastal Zone under Climate Change Scenarios**

3 Christos Makris¹, Panagiota Galiatsatou², Yannis Androulidakis³, Zisis Mal-
4 lios⁴, Vasilis Baltikas⁴, Yannis Krestenitis⁴

5 ¹ Democritus University of Thrace, Dept. of Civil Engineering, 67100 Xanthi,
6 Greece

7 ² EYATH S.A., 54621 Thessaloniki, Greece

8 ³ University of the Aegean, Dept. of Marine Sciences, 81100 Mytilene,
9 Greece

10 ⁴ Aristotle University of Thessaloniki, Dept. of Civil Engineering, 54124
11 Thessaloniki, Greece
12 cmakris@civil.duth.gr

13 **Abstract.** The intensifying threat of coastal flooding due to cli-
14 mate change calls for robust modelling and site-specific projec-
15 tions of extreme storm surge events combined with estimations of
16 Sea Level Rise (SLR) and astronomical tides. Greece, with over
17 15,000 km of coastline and several low-lying littoral zones, is par-
18 ticularly vulnerable to such hazards. This study aims to assess the
19 projected impact of climate change on the magnitude and fre-
20 quency of extreme storm surges across key coastal areas in Greece,
21 through the integration of a) large-scale modelled coastal sea level
22 dynamics and historical tide-gauge records, and b) high-resolution
23 Digital Terrain Models (DTM) and fine-scale hydraulic flood
24 modelling simulations. A hybrid methodology combining Ex-
25 treme Value Analysis (EVA) for storm-induced sea levels with
26 physics-based hydrodynamic inundation modelling
27 (CoastFLOOD) was applied across several exposed areas along
28 the Greek coasts. The case studies refer to both natural beaches in
29 low-lying rural coastal environments and engineered waterfronts
30 in urban areas. Coastal sea-level input for flood-hazard scenario
31 simulations was constructed using GEV-based return levels (e.g.,
32 50-, 100-year), including future SLR contributions and local char-
33 acteristics of astronomical tides, based on Representative Concen-
34 tration Pathways (RCP) 4.5 and 8.5. Graphical outputs include
35 maps of flood extents, characteristic floodwater depths and

36 velocities, inundation hazard indices, and climate change signals.
37 Our simulations reveal substantial increases in flood extent and
38 intensity under future scenarios, mainly affected by potentially in-
39 creasing SLR towards the end of the 21st century (2066-2100)
40 compared to a reference historical period (1971-2005), especially
41 in low-land urbanised zones. For the standard 100-year return
42 level of storm tides, combined with SLR, floodwater inundation is
43 projected to reach critical infrastructure, residential zones, and
44 transport pathways. Furthermore, a preliminary exposure assess-
45 ment indicates that coastal properties in certain areas may be af-
46 fected under worst-case scenarios, underscoring the need for up-
47 dated zoning and adaptive planning. These findings emphasise the
48 need for integrating future storm surge extremes into locally im-
49 plemented flood risk management, real estate and insurance valu-
50 ation, socioeconomic impact assessment, and protection schemes
51 in Greek coastal areas. The proposed methodological framework
52 provides a reproducible approach for similar evaluations in other
53 Mediterranean coastal regions facing flood threats.

54 **Keywords:** Coastal Inundation, Storm Surge, Sea Level Rise,
55 Extreme Value Analysis, Greece.

56 **1 Introduction**

57 Coastal zones worldwide are increasingly exposed to the combined effects of
58 mean sea-level rise (MSLR), changes in storminess, and anthropogenic pres-
59 sures. In semi-enclosed basins such as the Mediterranean Sea, storm surges and
60 wave storms, superimposed on rising mean sea level (MSL), can generate a
61 total water level (TWL) that may threaten coastal communities, critical infra-
62 structure, and ecosystems. Greece, with over 15,000 km of coastline and many
63 densely populated, low-lying littoral areas, is particularly vulnerable to episodic
64 coastal flooding driven by extreme storm-tide events.

65 Recent studies have shown that storm surge maxima in the Mediterranean
66 exhibit substantial regional variability due to complex basin geometry, variable
67 bathymetry, shifts in cyclogenesis centres, the distribution of cyclonic tracks,
68 and the influence of deep depressions [1]. At the same time, long-term changes
69 in storminess under climate change are not spatially uniform; several studies
70 report a general attenuation of surge extremes over large parts of the basin, but
71 with local increases at specific gulfs, bights, and coastal inlets [2]. Such nu-
72 anced patterns underscore the need for regional-to-local-scale assessments that
73 translate large-scale climate signals into site-specific coastal flood-hazard pro-
74 jections [3,4].

75 For the design of engineering flood protection and coastal risk management,
76 extreme total water levels with specified return periods are typically estimated
77 using Extreme Value Analysis (EVA) applied to historical or modelled sea-
78 level records. The Generalised Extreme Value (GEV) distribution and the
79 Peaks-Over-Threshold approach have been widely used in coastal applications
80 to estimate return levels of storm surge and wave heights [5,6]. In a changing
81 climate, however, the uncertainty is prevalent; thus, modelling chains must in-
82 tegrate ensemble climate projections with hydrodynamic and statistical meth-
83 ods to derive future design conditions at the shoreline.

84 In parallel, numerical modelling of overland flooding has advanced signifi-
85 cantly. While several complete shallow-water equation solvers provide full hy-
86 drodynamic simulations, reduced-complexity approaches (e.g., LISFLOOD
87 and SFINCS) based on rasterised, mass-balance, Manning-type formulations
88 have become very popular for large-scale applications, owing to their compu-
89 tational efficiency and ability to handle very high spatial-resolution digital ele-
90 vation models (DEMs) [7,8]. The CoastFLOOD model [9] belongs to this cat-
91 egory and has been applied to a range of coastal inundation problems in Greece
92 and the US.

93 This contribution presents a hybrid framework designed to quantify future
94 changes in extreme storm tides and associated coastal flooding along the Greek
95 coastal zone under selected climate change scenarios. The specific objectives
96 are to: (i) use atmospheric input from MED-CORDEX climate simulations
97 [10,11] as input to feed MeCSS model runs for storm surges/tides [1]; (ii) derive
98 ensemble projections of extreme sea levels at the shoreline based site-specific
99 EVA [12]; (iii) transform these drivers into high-resolution flood hazard maps
100 (extent, height, velocity, intensity) for several representative Greek coastal sites
101 using high-resolution CoastFLOOD model simulations [9]; (iv) synthesise the
102 results in terms of a Coastal Inundation Hazard Index (CIHI) ranking [13]; and
103 (v) discuss implications for climate-resilient coastal management.

104 **2 Methods and Data**

105 The proposed methodology integrates regional climate projections, storm surge
106 modelling, extreme value statistics, and reduced-complexity coastal flooding
107 simulations applied along the entire coastline of Greece, with a focus on 20
108 characteristic littoral regions across the Aegean, Ionian, and Cretan Seas. It pro-
109 ceeds in four main steps: (1) storm-surge simulations for the Mediterranean Sea
110 using the MeCSS model driven by Regional Climate Model (RCM) outputs;
111 (2) extraction of annual maxima for storm-induced Sea Surface Heights (SSH)
112 and EVA at littoral grid points along the Greek coasts; (3) construction of loca-
113 tion-specific total water-level scenarios by adding maximum astronomical tidal
114 ranges and projected MSLR; and (4) CoastFLOOD inundation simulations for

115 a set of representative Greek coastal sites under present and future extreme
116 forcing.

117 Storm surges are simulated using the Mediterranean Climate Storm Surge
118 (MeCSS) model, a depth-averaged barotropic hydrodynamic model based on
119 the shallow-water equations. MeCSS solves for water levels and depth-aver-
120 aged currents on a curvilinear grid covering the entire Mediterranean basin,
121 with open boundaries prescribed at the Strait of Gibraltar and Marmara [1]. At-
122 mospheric forcing consists of 10 m wind components and sea-level pressure
123 fields from three high-resolution Mediterranean Coordinated Regional
124 Downscaling Experiment (MED-CORDEX) RCMs:

- 125 • CMCC-CCLM: Euro-Mediterranean Centre on Climate Change (CMCC),
126 Climate Model COSMO-Climate Limited-area Modelling (CCLM)
- 127 • CNRM-ALADIN52: National Center for Meteorological Research (CNRM)
128 Aire Limitée Adaptation dynamique Développement InterNational (ALADIN)
- 129 • GUF-CCLM-NEMO: Goethe University of Frankfurt (GUF) CCLM – Nu-
130 cleus for European Modelling of the Ocean (NEMO)

131 Simulations are conducted for a historical reference period (1971–2005) and
132 two 35-year future periods (STF: 2021–2055; LTF: 2066–2100) under RCP4.5
133 and RCP8.5 [1, 10, 11]. For each coastal grid cell, the storm-induced SSH time
134 series is extracted and high-pass filtered to remove low-frequency signals not
135 related to meteorological forcing.

136 EVA is applied to the annual maximum storm-induced SSH series at each
137 littoral grid cell. The GEV distribution is selected because it represents the lim-
138 iting distribution of block maxima under general conditions [14]. The cumula-
139 tive distribution function is defined by the location parameter μ , the scale pa-
140 rameter σ , and the shape parameter ζ , which controls the tail behaviour. Param-
141 eter estimation is performed using the L-moments method, which has proven
142 robust for relatively short samples (here, 35 years of annual maxima per period)
143 [12]. For each cell, 50- and 100-year return levels of storm-induced SSH are
144 estimated. Confidence intervals are constructed using a parametric bootstrap
145 procedure in which synthetic samples are generated from the fitted GEV, re-
146 fitted, and return levels re-computed to obtain empirical percentiles.

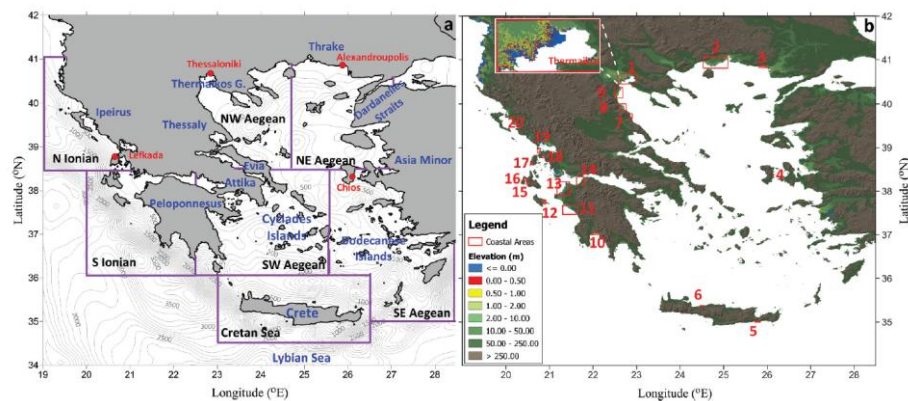
147 To combine storm surges with long-term MSLR, the derived storm-induced
148 SSH extremes are superimposed on projected MSL changes for the correspond-
149 ing RCP scenarios and periods. This yields location-specific TWLs that repre-
150 sent the combined effect of surges, tides, and MSL change. These TWLs are
151 used as offshore boundary conditions for local inundation simulations.

152 Coastal flooding is simulated using CoastFLOOD [9], a reduced-complexity
153 two-dimensional model that solves the mass conservation equation on a regular
154 raster grid. Water depths in each cell evolve according to the balance between
155 incoming and outgoing discharges to neighbouring cells and local storage. Hy-
156 draulic fluxes are computed using a decomposed Manning-type formulation
157 driven by water-level gradients between adjacent cells. The wetting–drying

158 algorithm activates or deactivates cells based on local water-depth thresholds.
 159 The computational domain covers coastal stretches of 1–20 km length and similar
 160 cross-shore extent, discretised at 2–5 m resolution, yielding simulation
 161 grids of up to about 16×10^6 cells.

162 The necessary DEMs are derived from the Hellenic Cadastre, which provides
 163 detailed topographic data for the coastal floodplains. Land-cover information is
 164 taken from CORINE Land Cover (CLC) datasets, which classify Europe into
 165 44 land-use categories. These categories are mapped to Manning roughness coefficients
 166 through look-up tables, and the resulting spatially variable friction fields are used to
 167 parameterise floodplain resistance to water flow. For each coastal site, scenarios of extreme
 168 storm-tide events are translated into time-varying boundary conditions applied along the seaward
 169 edge of the domain, and simulations are run for several hours to a few days to capture the potential
 170 maximum inundation buildup.
 171

172 Twenty representative coastal sites distributed across seven Greek regional seas are selected
 173 (Fig. 1): the northwestern, northeastern, southwestern, and southeastern Aegean Sea, the Cretan Sea,
 174 and the northern and southern Ionian Sea. Sites include both urbanised settings, such as Thessaloniki
 175 and the broader Thermaikos Gulf, Alexandroupolis, and Kalamata, and more rural or touristic
 176 locations, such as Laganas (Zakynthos), Vassiliki (Lefkada), and Ierapetra (Crete).
 177
 178



179
 180 **Fig. 1.** Bathymetry of the study area with 7 subregions and 20 locations at the
 181 NW Aegean, NE Aegean, SW Aegean, SE Aegean, Cretan Sea, N Ionian, and
 182 S Ionian Sea: Thermaikos Gulf (1), Nestos (2), Alexandroupolis (3), Chios (4),
 183 Ierapetra (Crete; 5), Rethymno (Crete; 6), Pineios (7), Agiokampos (8), Kate-
 184 rini (9), Kalamata (10), Katakolo (11), Laganas (Zakynthos; 12), Manolada
 185 (13), Patra (14), Argostoli (Kefalonia; 15), Livadi (Kefalonia; 16), Vassiliki
 186 (Lefkada; 17), Palairos (18), Preveza (19), Igoumenitsa (20).
 187

188 For each site and scenario, the spatial extent of flooding is extracted and nor-
 189 malised to a reference area (the global upper threshold of inundation area),

190 which serves as input to our coastal hazard analysis. The CIHI is defined as a
 191 composite metric combining a ranked driver-intensity term (based on the mag-
 192 nitude of the extreme TWL) with a ranked normalised flood-area term (the ratio
 193 of flooded area to a predefined ceiling):

$$194 \quad CIHI_j = FO_j \times \overline{FCP_{i,ext_j}} \quad (1)$$

195 where FCP is the daily Flood Coverage Percentage (%), FO is the Frequency
 196 of Occurrence (%) of the days with extreme $FCP_{i,j}$, overbar denotes the tem-
 197 poral mean, and i, j are indices of the number of days and the study area, re-
 198 spectively. CIHI values are used to categorise sites into low-, moderate-, and
 199 high-hazard classes under present and future conditions, and to quantify relative
 200 changes attributable to climate forcing.

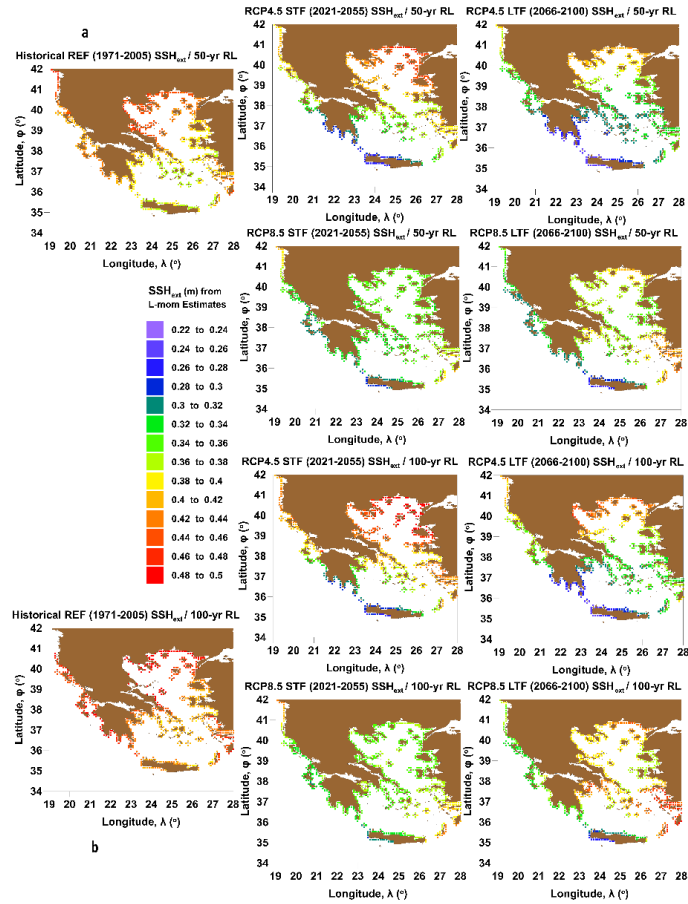
201 **3 Results**

202 **3.1 Extreme Storm Surges on the Coast**

203
 204 The GEV-based EVA of MeCSS storm-surge simulations confirms the sub-
 205 stantial spatial variability of extreme storm-induced SSH along the study area's
 206 coastline and, in particular, around Greece. For the historical reference period,
 207 the highest 50- and 100-year return levels in the wider Mediterranean are found
 208 in the northern Aegean. Along the Greek coasts, 50-year storm-surge return
 209 levels generally range from 0.25 to 0.55 m, with the highest values occurring at
 210 exposed gulfs with long fetches and favourable orientations relative to domi-
 211 nant winds (Fig. 2).

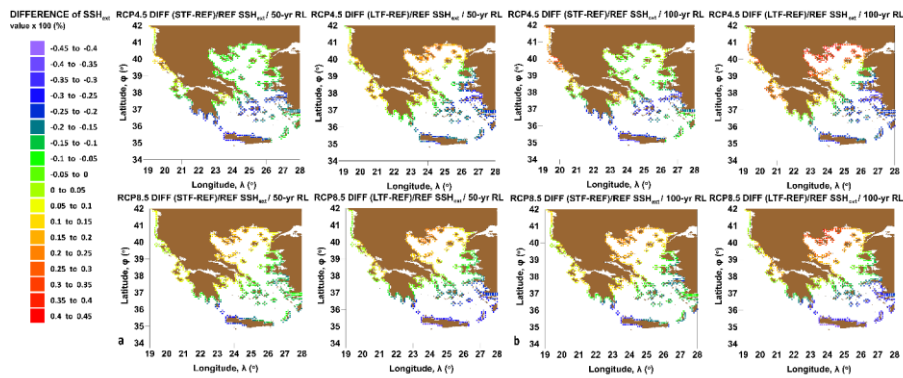
212 When comparing future periods with the reference baseline, a basin-wide
 213 attenuation of storminess is evident under both RCP4.5 and RCP8.5, particu-
 214 larly in the 2nd half of the 21st century (Fig. 3). Percentage differences in 50-
 215 year storm surges across the study area typically range from -30% to -2% by
 216 2100. Nonetheless, this overall decrease may mask a substantial positive local
 217 deviation in the central and northern Aegean and Ionian Seas; storm-surge ex-
 218 tremes may increase by up to 20–30%, depending on the RCM and scenario.

219 For Greece, the ensemble of MeCSS-RCM simulations reveals a mixed pat-
 220 tern. In several regions, particularly in the southern Aegean and parts of the
 221 Ionian Sea, the projected reduction in storminess is expected to slightly lower
 222 future surge extremes. In contrast, the northern Aegean, the entrance of Ther-
 223 maikos Gulf, and some Ionian sites display modest but statistically meaningful
 224 increases in extreme storm tides under at least one scenario-RCM combination.
 225 When combined with MSLR, even modest changes in surge extremes can trans-
 226 late into appreciable differences in TWLs at the coast.



227
228
229
230

Fig. 2. Maps of 50- & 100-year RV of Extreme SSH by GUF-based MeCSS simulations during Reference, STF, LTF for RCP 4.5-8.5.

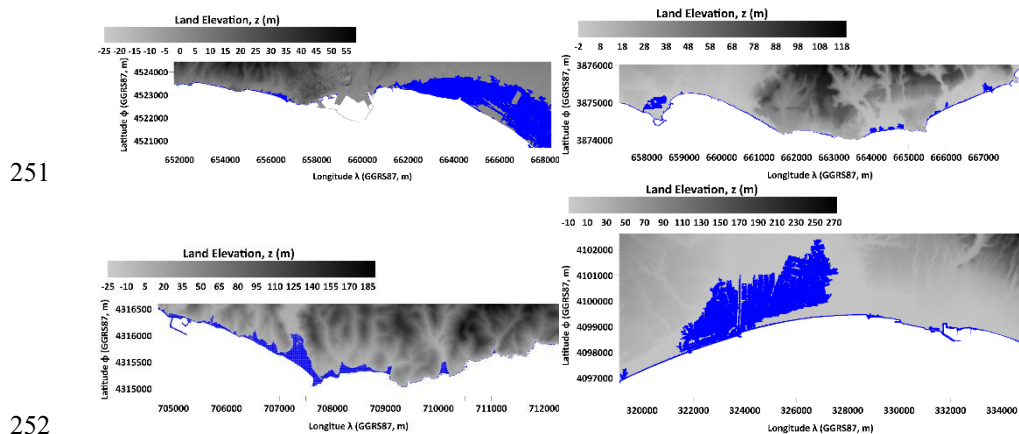


231
232
233

Fig. 3. Maps of Differences for 50- & 100-year RV of SSH_{ext} by CNRM-based MeCSS simulations during Reference STF and LTF for RCP4.5-8.5.

234 3.2 Coastal Flooding Impacts due to several TWL Scenarios

235 CoastFLOOD simulations driven by the highest projected total water levels
 236 translate these offshore signals into spatially explicit flood maps (Fig. 4). For
 237 Alexandroupolis, located in the northern Aegean, future scenarios under the
 238 RCP8.5 project a clear expansion of flood extent across low-lying urban areas
 239 near the port and the airport access roads, with flooded areas increasing by more
 240 than 15% relative to present-day conditions in the long term. In Ierapetra, on
 241 the southern coast of Crete, steep topography restricts inland penetration, so
 242 flood extents remain relatively limited despite elevated water levels, highlight-
 243 ing the crucial role of local morphology. In western Greece, simulations for
 244 Kalamata and Plomari illustrate different hydrodynamic behaviours. In
 245 Plomari, a narrow coastal lowland is easily over-topped under combined surge
 246 and MSLR, and floodwaters can propagate along the coastal plain, threatening
 247 transport corridors and built-up areas. Kalamata, by contrast, exhibits hydraulic
 248 connectivity between the shoreline and more inland depressions, so storm tides
 249 can activate complex flow pathways that inundate areas not directly adjacent to
 250 the sea.



252 **Fig. 4.** Flood Extents (FA) with CoastFLOOD simulations driven by the highest
 253 extreme TWL in Alexandroupoli (N Greece), Plomari (W Greece), Kalamata
 254 (SE Greece), Ierapetra (S Greece) from left to right and top to bottom.

255 At several sites, projected changes in the area affected by flooding under
 256 RCP8.5 by 2100 fall within the range of 10–20%, whereas in other locations
 257 they remain within a few per cent, consistent with local attenuation of stormi-
 258 ness.
 259

261 3.3 Results on Flood Hazard Management

262 CIHI provides a synthetic view of these results by ranking all 20 sites based
 263 on combined driver intensity and flood response. Under historical conditions,
 264 the highest CIHI values occur in low-lying deltas, embayments, and back-

265 barrier plains with extensive urbanisation or critical assets. In the long-term
 266 future under RCP8.5, several of these sites experience an upward shift in hazard
 267 class, while a few locations with currently moderate hazard move into the high-
 268 hazard category. Conversely, a limited number of sites with favourable topog-
 269 raphy and reduced storminess exhibit stable or slightly reduced CIHI values.

270 Overall, the analysis reveals that the combined effect of changing storm
 271 surges and sea-level rise is highly site-specific (Table 1). The spatially coherent
 272 patterns associated with atmospheric deep depressions and Mediterranean cy-
 273 clone tracks interact with local coastal morphology and land-use to produce a
 274 rich spectrum of future flood responses along the Greek coastline.

275

276 **Table 1.** Characteristic CIHI values for hazard severity by combining ranked
 277 driver (storm tide) intensity with a ranked Normalised Inundation Index
 278 (Flooded Fraction), $FA_{ext}/FA_{ceiling}$.

| A/A | Ierapetra | Rethymno | Kalamata | Katakolo | Argostoli | Livadi |
|------|-----------|----------|----------|----------|-----------|------------|
| MAX | 1.061 | 0.902 | 1.273 | 1.105 | 1.057 | 1.059 |
| RANK | 12 | 22 | 3 | 10 | 14 | 13 |
| CIHI | 5 | 5 | 1 | 5 | 1 | 1 |
| A/A | Patra | Chios | Vasiliki | Palairos | Plomari | Kyparissia |
| MAX | 1.105 | 0.974 | 1.042 | 1.055 | 1.222 | 1.138 |
| RANK | 11 | 18 | 16 | 15 | 5 | 7 |
| CIHI | 2 | 3 | 2 | 1 | - | - |

279 4 Discussion

280 The results confirm that climate change affects storm surges and coastal flood-
 281 ing in the Mediterranean in ways that simple monotonic trends cannot summa-
 282 rise. Instead, they emerge from a combination of (i) large-scale modifications
 283 in the frequency, intensity, and tracks of deep depressions and cyclones [15],
 284 (ii) regional sea-level rise [16], and (iii) local coastal morphology and human
 285 occupation [17,18]. The projected basin-wide attenuation of storm surges in
 286 many regions reflects a likely northward shift and reorganisation of atmos-
 287 pheric circulation patterns [1]. Yet, local hotspots of intensification persist,
 288 where topographic and bathymetric configurations favour surge amplification
 289 [13]. Specifically, a comparison of positive vs negative differences DIFF (%)
 290 in extreme Flood Extents (FA_{ext}) at selected Greek coastal sites is presented in
 291 Table 2, based on combinations of climatic scenarios, RCPs, RCMs, and Re-
 292 turn-Periods (RPs), e.g.:

$$293 \text{DIFF}(FA_{ext}) = (FA_{ext,RCP45-STF} - FA_{ext,Reference}) / FA_{ext,Reference} \quad (2)$$

294 Positive changes are few but, conditionally, exceed the 5% significance thresh-
 295 old. For infrastructure designers and coastal planners, this implies that relying
 296 solely on basin-average or global sea-level rise projections is insufficient for
 297 robust risk assessments [18]. Instead, detailed regional modelling of storm
 298 surges, combined with extreme-value statistics and high-resolution inundation
 299 simulations, is required to identify the most critical sites and quantify the range
 300 of possible future outcomes. The hybrid framework presented here offers such
 301 a pathway by linking MED-CORDEX RCM outputs, MeCSS surge simula-
 302 tions, EVA, and CoastFLOOD at representative Greek sites. The used FA_{ext}
 303 values are classified in Section 3.2's analysis of coastal inundation impacts due
 304 to several TWL, prioritised based on outputs similar to Fig. 4 for all case study
 305 areas, where positive changes in $DIFF(FA_{ext})$ prevail.

306

307 **Table 2.** Positive vs negative differences $DIFF$ (%) of extreme Flood Extents
 308 (FA_{ext}) from Eq. 2 at selected Greek coastal sites based on combinations of
 309 RCPs, RCMs, and RPs. Positive changes are marked in bold.

| RCP/ Future | RCM | RP (years) | Ierapetra | Rethymno | Kalamata | Laganas | Thermaikos |
|----------------|------|---------------|-----------|--------------|--------------|--------------|--------------|
| RCP45- STF | CMCC | 50 | -2.03% | 1.51% | -0.50% | 2.12% | 2.70% |
| | | 100 | 0.00% | 2.93% | -0.39% | 2.13% | 1.71% |
| | CNRM | 50 | -6.26% | -11.64% | -5.74% | -2.88% | -0.98% |
| | | 100 | -5.65% | -11.24% | -5.80% | -2.78% | 0.40% |
| | GUF | 50 | -11.47% | -10.51% | -7.82% | -8.14% | -1.17% |
| | | 100 | -11.55% | -13.97% | -9.13% | -12.45% | -2.15% |
| RCP45- LTF | CMCC | 50 | -4.15% | -5.42% | 0.77% | 3.48% | -1.41% |
| | | 100 | -3.05% | -6.33% | 1.17% | 5.01% | -3.23% |
| | CNRM | 50 | -12.88% | -8.51% | 0.14% | 3.21% | 4.51% |
| | | 100 | -11.20% | -10.42% | 1.19% | 5.40% | 8.82% |
| | GUF | 50 | -14.23% | -12.75% | -9.54% | -8.80% | -1.83% |
| | | 100 | -15.25% | -14.39% | -10.30% | -12.09% | -2.28% |

310

311 The proposed CIHI is a pragmatic tool for synthesising complex information
 312 into a form accessible to decision-makers. By combining ranked contributions
 313 from extreme total water levels and normalised flood extents, CIHI simplifies
 314 the communication of hazard severity and its evolution under climate change.
 315 However, CIHI should be interpreted alongside complementary indicators that
 316 capture exposure and vulnerability, such as population density, the economic
 317 value of assets, critical infrastructure, and ecosystem services, to derive com-
 318 prehensive risk indices [19].

319 From the perspective of the United Nations Sustainable Development Goals
 320 (SDGs), the findings have direct implications for SDG 11 (Sustainable Cities

321 and Communities) and SDG 13 (Climate Action). Coastal municipalities with
322 increasing CIHI values will need to integrate future storm-tide-driven flood
323 hazards into spatial planning, building codes, emergency preparedness, and in-
324 surance schemes. Adaptation options may range from nature-based solutions,
325 such as wetland restoration and beach nourishment, to engineered defences and
326 managed retreat in the most exposed locations. The analysis also supports SDG
327 9 (Industry, Innovation and Infrastructure) by providing the quantitative basis
328 for climate-resilient design of ports, transport links, and water-related infra-
329 structure along the Greek coastline [20].

330 The study has several limitations that point to future research needs. First,
331 while the GEV-based EVA assumes stationarity within each 35-year window,
332 non-stationary approaches that explicitly incorporate time-varying covariates
333 could provide additional insight, especially for mid- to long-term planning. Sec-
334 ond, the analysis focuses on storm surges and mean sea-level rise, whereas
335 wave setup, runup, and coincident river discharges are treated implicitly or ne-
336 glected. Extending the framework to account for fully coupled flooding by in-
337 tegrating coastal surge and waves with fluvial and pluvial models would yield
338 a more comprehensive representation of coastal compound flood hazards.
339 Third, uncertainties associated with climate model ensembles, emission path-
340 ways, and local topographic data should be quantified more explicitly through
341 systematic sensitivity and probabilistic analyses.

342 Despite these limitations, the present work demonstrates the feasibility and
343 value of downscaling Mediterranean-scale climate information to the local
344 scale of individual Greek coastal communities. The combination of physically
345 based modelling and statistical analysis provides a consistent framework that
346 can be updated as new climate scenarios, RCM simulations, and higher-quality
347 topographic data become available.

348 **5 Conclusions**

349 A hybrid framework has been presented to assess future extreme storm tides
350 and associated coastal flooding along the Greek coastal zone under climate
351 change scenarios. The approach combines MED-CORDEX climate projec-
352 tions, MeCSS storm-surge simulations, GEV-based EVA, and reduced-com-
353 plexity CoastFLOOD inundation modelling at high spatial resolution for twenty
354 representative Greek coastal sites.

355 The results indicate that, while a general attenuation of storm surges is pro-
356 jected over large parts of the Mediterranean basin by the end of the twenty-first
357 century, several Greek hotspots may experience local increases in extreme
358 storm-tide levels and flood extents when storm surges are superimposed on
359 mean sea-level rise. Projected changes in flood impacts range from negligible

360 to more than 20% under RCP8.5 in the long term (not shown here for brevity),
361 depending on location, coastal morphology, and atmospheric forcing.

362 The Coastal Inundation Hazard Index (CIHI) introduced in this study pro-
363 vides a valuable synthesis of driver intensities and flood responses, offering a
364 transparent means to compare hazard levels across sites and scenarios. The
365 methodology and results can directly support coastal risk assessments, adapta-
366 tion strategies, and investment planning aligned with the objectives of SDGs 9,
367 11, and 13.

368 Future work will focus on extending the framework to fully account for com-
369 pound flooding, incorporating wave effects and river discharge, refining non-
370 stationary statistical models of extremes, and integrating exposure and vulner-
371 ability data to derive comprehensive coastal risk indices for Greece and the
372 wider eastern Mediterranean.

373 **References**

- 374 1. Makris, C.V., Tolika, K., Baltikas, V.N., Velikou, K., Krestenitis, Y.N.:
375 The impact of climate change on the storm surges of the Mediterranean Sea:
376 coastal sea level responses to deep depression atmospheric systems. *Ocean*
377 *Modelling* 181, 102149 (2023).
- 378 2. Conte, D., Lionello, P.: Characteristics of large positive and negative surges
379 in the Mediterranean Sea and their attenuation in future climate scenarios.
380 *Global and Planetary Change* 111, 159–173 (2013).
- 381 3. Lionello, P., Conte, D., Reale, M.: The effect of cyclones crossing the Med-
382 iterranean region on sea level anomalies on the Mediterranean Sea coast.
383 *Natural Hazards and Earth System Sciences* 19(7), 1541–1564 (2019).
- 384 4. Šepić, J., Vilibić, I., Jordà, G., Marcos, M.: Mediterranean sea level forced
385 by atmospheric pressure and wind: variability of the present climate and
386 future projections for several period bands. *Global and Planetary Change*
387 86, 20–30 (2012).
- 388 5. Calafat, F.M., Wahl, T., Tadesse, M.G., Sparrow, S.N.: Trends in Europe
389 storm surge extremes match the rate of sea-level rise. *Nature* 603, 841–845
390 (2022).
- 391 6. Cid, A., Menéndez, M., Castanedo, S., Abascal, A.J., Méndez, F.J., Medina,
392 R.: Long-term changes in the frequency, intensity and duration of extreme
393 storm surge events in southern Europe. *Climate Dynamics* 46(5), 1503–
394 1516 (2016).
- 395 7. Sharifian, M. K., Kesserwani, G., Chowdhury, A. A., Neal, J., Bates, P.:
396 LISFLOOD-FP 8.1: New GPU accelerated solvers for faster fluvial/pluvial
397 flood simulations. *Geoscientific Model Development Discussions* 16(9),
398 2391–2413 (2023).

- 399 8. Leijnse, T., van Ormondt, M., Nederhoff, K., & van Dongeren, A.: Model-
400 ing compound flooding in coastal systems using a computationally efficient
401 reduced-physics solver: Including fluvial, pluvial, tidal, wind-and wave-
402 driven processes. *Coastal Engineering* 163, 103796 (2021).
- 403 9. Makris, C., Mallios, Z., Androulidakis, Y., Krestenitis, Y.: CoastFLOOD:
404 A High-Resolution Model for the Simulation of Coastal Inundation Due to
405 Storm Surges. *Hydrology*, 10(5), 103 (2023).
- 406 10. Ruti, P.M., et al.: MED-CORDEX initiative for Mediterranean climate
407 studies. *Bulletin of the American Meteorological Society* 97(7), 1187–1208
408 (2016).
- 409 11. Reale, M., Cabos Narvaez, W.D., Cavicchia, L., Conte, D., Coppola, E.,
410 Flaounas, E., Giorgi, F., Gualdi, S., et al.: Future projections of Mediterra-
411 nean cyclone characteristics using the Med-CORDEX ensemble of coupled
412 regional climate system models. *Climate Dynamics*, 1–24 (2021).
- 413 12. Galiatsatou, P., Makris, C., Baltikas, V., Krestenitis, Y., Prinos, P.: Analy-
414 sis of extreme storm surges at the Mediterranean coastline under climate
415 change. In Karambas T., Loukogeorgaki, E. (eds.) 2nd International Scien-
416 tific Conference on Design and Management of Port Coastal and Offshore
417 Works (DMPCO), vol. 1, pp. 36-40 (2023).
- 418 13. Androulidakis, Y., Makris, C., Mallios, Z., Krestenitis, Y.: Sea level varia-
419 bility and coastal inundation over the northeastern Mediterranean Sea.
420 *Coastal Engineering Journal*, 65(4), 514-545 (2023).
- 421 14. Coles, S.: *An Introduction to Statistical Modeling of Extreme Values*.
422 Springer, London (2001).
- 423 15. Androulidakis, Y., Makris, C., Mallios, Z., Pytharoulis, I., Baltikas, V.,
424 Krestenitis Y.: Storm surges and coastal inundation during extreme events
425 in the Mediterranean Sea: the IANOS Medicanne. *Natural Hazards* 117(1)
426 939-978 (2023).
- 427 16. Velegrakis, A.F. et al.: Coastal Hazards and Related Impacts in Greece. In:
428 Darques, R., Sidiropoulos, G., Kalabokidis, K. (eds.) *The Geography of*
429 *Greece*. World Regional Geography Book Series. Springer, Cham. (2024).
- 430 17. Giannakidou, C., Diakoulaki, D., Memos, C.D.: Vulnerability to Coastal
431 Flooding of Industrial Urban Areas in Greece. *Environmental Processes*. 7,
432 749–766 (2020).
- 433 18. Roukounis, C.N., Tsoukala, V.K., Tsihrintzis, V.A.: An Index-Based
434 Method to Assess the Resilience of Urban Areas to Coastal Flooding: The
435 Case of Attica, Greece. *Journal of Marine Science and Engineering*,
436 11(9):1776 (2023).
- 437 19. Malliouri, D., Petrakis, S., Fadin, L. et al.: The coastal flooding risk
438 throughout the twenty-first century at the ancient city of Delos, Greece.
439 *Natural Hazards* 121, 11829–11854 (2025).
- 440 20. Monioudi, I.N., Chatzistratis, D., Moschopoulos, K., Velegrakis, A.F., Pol-
441 ydoropoulou, A., Chalazas, T., Bouhouras, E., Papaioannou, G., Karakikes,

442 I. and Thanopoulou, H.: Exposure of Greek Ports to Marine Flooding and
443 Extreme Heat Under Climate Change: An Assessment. *Water*, 17(13), 1897
444 (2025).